Inorganic Chemistry

ARTICLE

pubs.acs.org/IC

Reversible Fluorescent Probe for Highly Selective and Sensitive Detection of Mercapto Biomolecules

Jiasheng Wu, Ruilong Sheng, Weimin Liu, Pengfei Wang,* Jingjin Ma, Hongyan Zhang, and Xiaoqing Zhuang

Key Laboratory of Photochemical Conversion and Optoelectronic Materials, Technical Institute of Physics and Chemistry, Chinese Academy of Sciences, Beijing 100190, People's Republic of China

Supporting Information

ABSTRACT: A coumarin-derived complex, $\mathbf{Hg_2L_2}$, was reported as a highly sensitive and selective probe for the detection of mercapto biomolecules in aqueous solution. The addition of Cys to a 99% aqueous solution of $\mathbf{Hg_2L_2}$ resulted in rapid and remarkable fluorescence *OFF*−*ON* (emission at 525 nm) due to the ligand-exchange reaction of Cys with **L** coordinated to Hg^{2+}. The increased fluorescence can be completely quenched by Hg^{2+} and recovered again by the subsequent addition of Cys. Such a fluorescence *OFF*−*ON* circle can be repeated at least 10 times by the alterative addition of Cys and Hg^{2+} to the solution of $\mathbf{Hg_2L_2}$, indicating that it can be used as a convertible and reversible probe for the detection of Cys. The interconversion of $\mathbf{Hg_2L_2}$ and **L** via the decomplexation/complexation by the modulation of Cys/Hg^{2+} was definitely verified from their crystal structures. Other competitive amino acids without a thiol group cannot induce any fluorescence changes, implying that $\mathbf{Hg_2L_2}$ can selectively determine mercapto biomolecules. Using confocal fluorescence imaging, $\mathbf{L}/\mathbf{Hg_2L_2}$ as a pair of reversible probes can be further applied to track and monitor the self-detoxification process of Hg^{2+} ions in SYS5 cells.

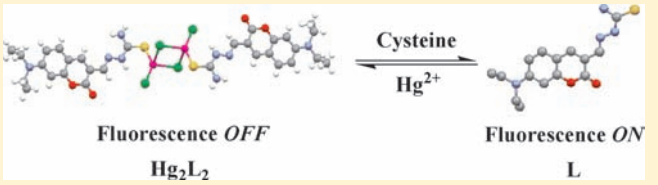

1. INTRODUCTION

Mercapto biomolecules, such as cysteine (Cys), homocysteine (Hcy), and glutathione (GSH), play a crucial role in maintaining biological systems.[1−3] Cys deficiency is involved in many syndromes including neurotoxicity, edema, liver damage, and hair depigmentation.[1] An elevated level of Hcy in plasma is a risk factor for neural tube defects, osteoporosis, and Alzheimer's and cardiovascular diseases.[2] GSH, as the most abundant intracellular nonprotein thiol, plays a pivotal role in maintaining the reductive environment in cells and acts as the redox regulator.[3] Because of its important role in biological systems, much attention has been paid to the detection of mercapto biomolecules. Many analytical techniques, including UV−vis detection assays, mass spectrometry (MS),[4] gas chromatography,[5] high-performance liquid chromatography,[6] and electrochemical methods,[7] have been available techniques, fluorescent probes have been widely used to sense mercapto biomolecules because of their simplicity, high selectivity, and sensitivity. Currently, a number of thiol-reactive fluorescent probes have been reported.[8] However, most of these probes are generally irreversible and thus remain in living cells, which will cause some negative impacts on cells, such as restricting further intracellular imaging of the desired analytes, preventing an understanding of the detailed interaction process in cells, and imparting possible damage to cells.[9] This requires a reversible fluorescent probe that can control the toxic/detox process to avoid toxic cellular uptake. As a result, it is highly desirable to develop reversible fluorescent probes for the sensitive and selective determination of mercapto biomolecules.

Fluorescein/rhodamine-based fluorescent probes have been receiving considerable attention because of their self-modulation of *OFF*−*ON* fluorescence, good water solubility, and longer emission wavelength (over 500 nm).[10] In view of their attractive advantages, there is still a high demand to develop new fluorophores with such properties. As we notice, coumarin derivatives as important fluorescent dyes are commonly considered to give rise to strong emission only in organic solvents.[11] In aqueous solution, the emission quantum yield is drastically decreased as a result of solvation. In addition, the poor solubility and relatively shorter emission wavelength (often below 500 nm) of conventional coumarin dyes also restrict their practical applications, especially in biological systems.[12] In this work, we developed a new coumarin-based imine, **L**, bearing an aminothiourea unit with an extensively green emission (Figure 1). Compared with conventional coumarin dyes, both 7-diethylamino and imine units in **L** extended the conjugation structure of the fluorophore. The aminothiourea unit was incorporated into **L** to increase its water compatibility and emitting ability in the hydrophilic environment. As expected, **L** gives rise to an extensive emission at 525 nm in aqueous solution with a quantum yield of 0.50. The emission can be completely quenched (over 98%) by 1 equiv of Hg^{2+} and recovered again (over 95%) with the addition of Cys. Both **L** and its complex with Hg^{2+} exhibit good stabilities under a wide pH span from 6 to 10, covering physiological conditions. These properties of **L** including high water solubility, longer

Received: January 26, 2011
Published: June 21, 2011

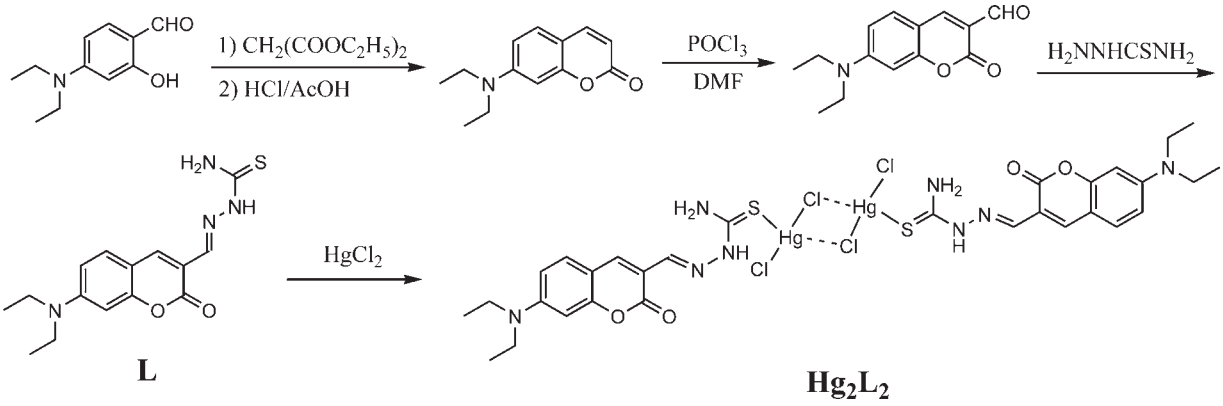

Figure 1. Synthetic pathway of ligand **L** and complex $\mathbf{Hg_2L_2}$.

emission wavelength (525 nm), and fluorescence *OFF*−*ON* to the guests are comparable with those of fluorescein/rhodamine-based fluorescent probes.[10]

With excellent properties of **L** in hand, herein, we further developed the complex $[\mathbf{Hg_2L_2}]^{4+}\mathbf{Cl_4}^-$ (abbreviated as $\mathbf{Hg_2L_2}$ in the text, vide infra) as a convertible fluorescent probe, which exhibited high sensitivity and selectivity to mercapto biomolecules via a reversible decomplexation (Figure 1). Interconversion of $\mathbf{Hg_2L_2}$ and **L** can repeatedly occur and is thus applied for the reversible fluorescent determination of mercapto biomolecules, such as Cys, Hcy, and GSH. Confocal fluorescence imaging reveals that $\mathbf{L}/\mathbf{Hg_2L_2}$ can be applied to monitor the intracellular self-detoxification of foreign Hg^{2+} ions in SYS5 cells.

2. EXPERIMENTAL SECTION

Instruments. ^{1}H and ^{13}C NMR spectra were recorded on an Advance Bruker instrument (400 MHz). UV−vis absorption and fluorescence spectra were recorded on a Hitachi U-3010 spectrometer and a Hitachi F-4500 fluorescence spectrometer, respectively. X-ray analysis was measured on a Rigaku R-Axis Rapid IP diffractometer. Mass spectra were recorded on a Finigan 4021C MS-spectrometer. High-resolution MS (HRMS) was recorded on a Bruker Daltonics Inc. APEX II FT-ICR mass spectrometer. Elemental analysis was measured on a FLASH EA1112 instrument.

Synthesis. 7-(*N*,*N*-Diethylamino)coumarin and 7-(*N*,*N*-diethylamino)coumarin-3-aldehyde were synthesized according to published procedures.[13]

*(E)-2-[[7-(Diethylamino)-2-oxo-2H-chromen-3-yl]methylene]hydrazinecarbothioamide (Ligand **L**).* To 7-(*N*,*N*-diethylamino)coumarin-3-aldehyde (250 mg, 1 mmol) dissolved in 20 mL of ethanol was added dropwise thiosemicarbazone (140 mg, 1.25 mmol) in 10 mL of ethanol. After the reaction refluxed for 5 h, orange crystals precipitated out. The needle crystals were collected and washed with ethanol (259 mg, yield 75%). ^{1}H NMR (400 MHz, DMSO-d_6, δ): 11.53 (s, 1H, NH), 8.65 (s, 1H, CH═N), 8.24 (s, 1H, ArH), 8.06 (s, 1H, NH), 8.01 (s, 1H, NH), 7.42 (d, J = 8.8 Hz, 1H, ArH), 6.78 (d, J = 7.2 Hz, 1H, ArH), 6.57 (d, J = 6.8 Hz, 1H, ArH), 3.48 (t, J = 6.8 Hz, 4H, CH_2), 1.15 (t, J = 6.8 Hz, 6H, CH_3). ^{13}C NMR (100 MHz, DMSO-d_6, δ): 177.6, 160.7, 156.4, 151.2, 138.9, 136.5, 130.3, 112.7, 109.8, 108.2, 96.5, 44.3, 12.4. ESI-MS ($[\mathbf{L} + H]^+$, m/z): 319.1 (calcd 319.1). ESI-HRMS ($[\mathbf{L} + H]^+$, m/z): 319.1219 (calcd 319.1223). Anal. Calcd for $C_{15}H_{18}N_4O_2S$: C, 56.58; H, 5.70; N, 17.60. Found: C, 56.58; H, 5.71; N, 17.72.

*Mercury Complex **Hg_2L_2**.* To a solution of **L** (320 mg, 1 mmol) dissolved in 5 mL of *N*,*N*-dimethylformamide (DMF)/EtOH (1:1, v/v) was added dropwise within 20 min 10 mL of $HgCl_2$ (400 mg, 1.5 mmol) in ethanol. An orange solid immediately precipitated out. After the solution was kept at 50 °C for another 10 h, the crude product was collected and washed with a small amount of ethanol (504 mg, yield 70%). ^{1}H NMR (400 MHz, DMSO-d_6, δ): 12.55 (s, 1H, NH), 9.31 (s, 1H, NH), 9.12 (s, 1H, NH), 8.65 (s, 1H, CH═N), 8.22 (s, 1H, ArH), 7.41 (d, J = 8.9 Hz, 1H, ArH), 6.80 (d, J = 7.6 Hz, 1H, ArH), 6.58 (d, J = 8.0 Hz, 1H, ArH), 3.48 (t, J = 6.8 Hz, 4H, CH_2), 1.15 (t, J = 6.8 Hz, 6H, CH_3). ^{13}C NMR (100 MHz, DMSO-d_6, δ): 166.5, 160.6, 157.1, 152.1, 144.7, 140.9, 131.0, 110.7, 110.3, 108.0, 96.6, 44.5, 12.5. ESI-MS ($[\mathbf{Hg_2L_2} + H]^+$, m/z): 1182.7 (calcd 1180.9). Anal. Calcd for $C_{30}H_{36}Cl_4Hg_2N_8O_4S_2$: C, 30.54; H, 3.08; N, 9.50. Found: C, 30.45; H, 3.10; N, 9.54.

Crystal Structure. Crystal data and details of the data collection are provided in Table 1. Diffraction data for **L** and $\mathbf{Hg_2L_2}$ were collected on a Bruker SMART D8 goniometer with an APEX CCD detector, using Mo Ka radiation λ = 0.710 73 Å (graphite monochromator). The structures were solved by direct methods (*SHELXTL*) and refined on F^2 by full-matrix least-squares techniques.[14] Hydrogen atoms were included by using a riding model. CCDC 783478 (**L**) and CCDC 783479 ($\mathbf{Hg_2L_2}$) contain the supplementary crystallographic data for this paper. These data can be obtained free of charge from the Cambridge Crystallographic Data Centre via www.ccdc.cam.ac.uk/data_request/cif.

Spectral Measurement. **L** (319 mg, 1 mmol) and $\mathbf{Hg_2L_2}$ (590 mg, 0.5 mmol) were dissolved in 1 mL of dimethyl sulfoxide (DMSO) or DMF and then diluted in a buffer solution (10 mM Tris-HCl, pH = 7.6) to 10 μM as the stock solution. The stock solutions of Cys, Hcy, GSH, and other competitive amino acids (1 mM) were prepared in a Tris buffer (10 mM Tris-HCl, pH = 7.6). These solutions were all kept at about 4 °C for further determination.

Fluorescence quantum yields were determined by comparing the emission integral area of the sample with that of a fluorescence standard by the following equation:

$$\Phi_U = \Phi_R \left(\frac{A_U}{A_R}\right)\left(\frac{{n_U}^2}{{n_R}^2}\right)$$

where A_U and A_R are the integrated areas under the corrected fluorescence spectrum for the sample and reference, respectively, n_U and n_R are the refractive indices of the sample and reference, respectively. The fluorescence quantum yield of the standard compound of fluorescein in 0.1 N NaOH aqueous solutions is 0.85.[15]

Cell Culture. HEK293 and SYS5 cell lines were prepared from a continuous culture in MEM, mixed with 10% (v/v) fetal bovine serum and 1% penicillin/streptomycin, at 37 °C in 5% CO_2 humidified air. Following cell adhesion (24 h), the cell culture medium was removed. After the cell was digested with trypsin, 1.0 mL of the cell suspension was transferred and incubated in cell walls of the microplate at 37 °C in 5% CO_2 humidified air for 24 h. The cell layer was washed twice with

dx.doi.org/10.1021/ic200181p |*Inorg. Chem.* 2011, 50, 6543–6551

Table 1. Crystal Data and Structure Refinement for Ligand L and Complex Hg_2L_2

compound	L	Hg_2L_2
empirical formula	$C_{19}H_{30}N_4O_4S_3$	$C_{30}H_{36}Cl_4Hg_2N_8O_4S_2$
fw	474.65	1179.79
temperature (K)	296(2)	296(2)
wavelength (Å)	0.710 69	0.710 73
cryst syst	triclinic	triclinic
space group	$P\bar{1}$	$P\bar{1}$
unit cell dimens	a = 7.1206(14) Å, α = 107.73(3)°, b = 12.751(3) Å, β = 99.35(3)°, c = 14.523(3) Å, γ = 99.80(3)°	a = 8.2194(16) Å, α = 97.93(3)°, b = 9.3156(19) Å, β = 105.24(3)°, c = 13.358(3) Å, γ = 94.29(3)°, 970.8(3) Å^3
volume (Å^3)	1204.9(4)	970.8(3)
Z, calcd density (Mg/m^3)	2, 1.308	1, 2.018
abs coeff (mm^{-1})	0.339	8.326
F(000)	504	564
θ range (deg)	2.65−25.00	2.22−27.48
limiting indices	$-8 \le h \le 8$, $-15 \le k \le 15$, $-17 \le l \le 17$	$-10 \le h \le 10$, $-12 \le k \le 12$, $-17 \le l \le 17$
reflns collected/unique	7847/4244 [R(int) = 0.0291]	8055/4440 [R(int) = 0.0593]
completeness to theta	25.00 (99.9%)	27.48 (99.6%)
abs corrn	semiempirical from equivalents	semiempirical from equivalents
max and min transmn	0.9605 and 0.8906	0.7883 and 0.2121
refinement method	full-matrix least squares on F^2	full-matrix least squares on F^2
data/restraints/param	4244/70/301	4440/0/226
GOF on F^2	1.108	0.989
final R indices [$I > 2\sigma(I)$]	R1 = 0.0614, wR2 = 0.1238	R1 = 0.0624, wR2 = 0.1529
R indices (all data)	R1 = 0.0912, wR2 = 0.1338	R1 = 0.0905, wR2 = 0.1656
largest diff peak/hole (e/Å^3)	0.304/−0.186	1.236/−1.498

phosphate-buffered saline (PBS), and then 1.0 mL of PBS was added in each well for fluorescence imaging.

Confocal Imaging. HEK293 and SYS5 cells were incubated with ligand **L** or complex $\mathbf{Hg_2L_2}$ (10 μM) for several minutes at room temperature. After the cell layer was carefully washed twice with PBS, the fluorescence emission was imaged using a Nikon confocal microscope. The excitation wavelength of the laser was 408 nm, and the emission was recorded at 515 nm. The same procedures were repeated when SYS5 cells were continuously treated with 100−300 μM $HgCl_2$ or Cys. *EZ-C1 3.20* free viewer was used as a platform for data analysis.

3. RESULTS AND DISCUSSION

Synthesis and Crystal Structure. Ligand **L** is a coumarin-based Schiff base synthesized from condensation of 7-(*N*, *N*-diethylamino)coumarin-3-aldehyde and aminothiourea (Figure 1). Complex $\mathbf{Hg_2L_2}$ was obtained from the coordination reaction of ligand **L** and $HgCl_2$ in an ethanol/DMF solvent mixture. X-ray block crystals were grown from the vapor diffusion of ether into an ethanol/DMF solution (10% DMF). ORTEP diagrams of **L** and $\mathbf{Hg_2L_2}$ are depicted in Figure 2, and the crystallographic data and selected geometric parameters are also given in Tables 1 and 2. **L** exists as an S-trans-type Schiff base chain with a thiocarbonyl group extended out of the coumarin ring (Figure 2a). From the dihedral angles of **L**, all atoms of aminothiourea in **L** were located almost in the same plane. It is also found that the dihedral angle between the coumarin-ring and aminothiourea planes is 179.9°, indicating that the whole molecule in **L** except for the diethylamino group has an excellent coplanar configuration. Thus, its emission ability is extensively increased. However, when bound with Hg^{2+}, **L** and Hg^{2+} can form a 2 + 2 complex with a chlorine-bridged structure. From Figure 2b, $\mathbf{Hg_2L_2}$ is a dimer structure in which ligand **L** serves as a monodentate to form Hg−S bonding. The coordination of Hg^{2+} is completed by a sulfur atom, a terminated chlorine atom, and two bridging chlorine atoms. Two mercury atoms and two chlorine atoms form a parallelogram configuration, and two Hg−S bonds are almost vertical to this parallelogram (the dihedral angels are 99.3° and 105.2°, respectively). The distance of two mercury atoms is 3.773(13) Å, and the bond length of Hg−S is 2.411(3) Å. In addition, some slight conformational changes of ligand **L** are observed when bound with Hg^{2+} (Table 2), indicating that the bound **L** still keeps a similar coplanar structure. As a result, complex $\mathbf{Hg_2L_2}$ is composed of three paralleling planes (two **L** planes and a Hg−Cl−Hg−Cl plane), and the distance of each plane is 2.411(3) Å. Three planes are linked by two Hg−S bonds, which are vertical to these planes. The formed structure can be explained by the soft and hard acids and bases.[16] According to the Irving−Williams rule, the sulfur and chlorine atoms belong to the soft base, while the oxygen and nitrogen atoms in **L** are the hard base. Thus, Hg^{2+}, as a soft acid, can be superior to bind with sulfur and chlorine atoms to form a more stable dimer structure in Figure 2b.

Absorption and Fluorescence Behaviors. Generally, imine-derived molecules are difficult to directly design as probes because of their instability upon irradiation and/or in acidic/

dx.doi.org/10.1021/ic200181p |*Inorg. Chem.* 2011, 50, 6543–6551

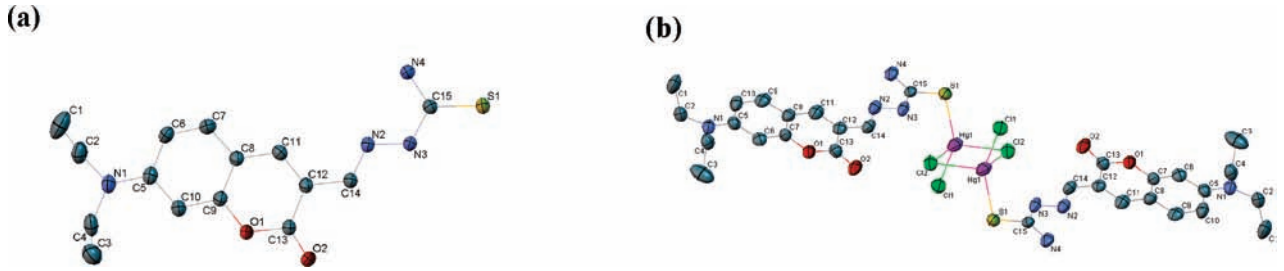

Figure 2. ORTEP diagrams of (a) ligand **L** and (b) complex Hg_2L_2 with displacement atomic ellipsoids drawn at the 30% probability level. Hydrogen atoms are omitted for clarity.

Table 2. Selected Interatomic Distances [Å] and Bond Angles [deg]

	L	Hg_2L_2		L	Hg_2L_2
Hg1−Cl1		2.385(3)	Cl2−Hg1−Cl2#1		91.62(8)
Hg1−S1		2.411(3)	Cl1−Hg1−Hg1#1		109.59(9)
Hg1−Cl2		2.562(3)	S1−Hg1−Hg1#1		106.57(8)
Hg1−Cl2#1		2.843(3)	Cl2−Hg1−Hg1#1		48.88(7)
Hg1−Hg1#1		3.773(13)	Cl2#1−Hg1−Hg1#1		42.75(5)
Cl2−Hg1#1		2.843(3)	Hg1−Cl2−Hg1#1		88.38(8)
S1−C15	1.691(3)	1.731(9)	C13−O1−C7	122.8(2)	122.7(8)
O1−C13	1.376(3)	1.364(11)	C14−N2−N3	116.3(2)	115.3(8)
O1−C7	1.383(3)	1.381(11)	C15−N3−N2	119.6(2)	118.6(8)
O2−C13	1.198(3)	1.233(12)	C6−C5−C10	117.7(3)	118.0(9)
N2−C14	1.271(4)	1.275(13)	C7−C6−C5	121.5(3)	119.7(9)
N2−N3	1.370(3)	1.392(11)	C11−C12−C14	123.5(3)	124.9(9)
N3−C15	1.342(4)	1.310(12)	C11−C12−C13	119.8(3)	119.4(9)
N4−C15	1.320(4)	1.295(11)	C14−C12−C13	116.7(3)	115.7(8)
C11−C12	1.366(4)	1.350(13)	O2−C13−O1	116.2(3)	117.4(9)
C12−C14	1.446(4)	1.443(13)	O2−C13−C12	126.7(3)	125.0(9)
C12−C13	1.455(4)	1.458(13)	O1−C13−C12	117.1(3)	117.5(8)
Cl1−Hg1−Cl2		112.80(9)	N2−C14−C12	121.1(3)	121.2(8)
S1−Hg1−Cl2		104.80(9)	N4−C15−N3	117.8(3)	120.9(9)
Cl1−Hg1−Cl2#1		95.50(10)	N4−C15−S1	122.9(2)	118.6(7)
S1−Hg1−Cl2#		98.53(10)	N3−C15−S1	119.4(2)	120.6(7)

basic solution. In a summary of previous literatures, most unstable imine intermediates were reduced to the corresponding amines for fluorescent sensing.[17] In this work, we found that coumarin-derived imine and its complex, **L**/Hg_2L_2, were stable enough even within a wide pH range (6−10). Because of the structural differences of **L** and Hg_2L_2, their photophysical properties are thus remarkably varied (Table 3). Ligand **L** displays a characteristic absorption band peaked at 452 nm (ε = 5.3 × 10^4 M^{-1} cm^{-1}) in a 99% aqueous solution. Upon the addition of Hg^{2+}, a distinct decrease in the absorbance at 452 nm and three obvious isosbestic points at 333, 375, and 497 nm were observed, as shown in Figure 3a. Corresponding to its absorption spectra, **L** gave an intensive emission band at 525 nm and its fluorescence was completely quenched (over 98%) immediately upon the addition of 1 equiv of Hg^{2+} (Figure 3b). The quantum yields of free ligand **L** and Hg^{2+}-bound forms were determined to be 0.50 and 0.031, respectively.[15] From Job's plot (inset of Figure 3b) and electrospray ionization (ESI; Figure S2 in the Supporting Information) analyses, the stoichiometric ratio of **L** with Hg^{2+} appeared to be 2:2, which was consistent with its crystal structure.

Table 3. Photophysical Properties of L and Hg_2L_2 in DMSO/H_2O (1:99, v/v)

compound	absorption λ_{max} (nm)	emission λ_{max} (nm)	ε (M^{-1} cm^{-1})	Stokes shift (nm)	quantum yield (Φ_f)
L	452	525	5.3 × 10^4	73	0.50
Hg_2L_2	450	521	3.0 × 10^4	71	0.031

It is generally believed that, in most fluorescent molecules, the introduction of an extended conjugation structure to the rigid aryl ring will result in a red shift of the emission wavelength, as well as a drastic decrease of the fluorescent quantum yield because of its weaker coplanar effect.[18] However, in our sensor **L**, the extended conjugation structure (aminothiourea group) well sites the same plane with the coumarin ring (Figure 2a). Thus, both the emission wavelength and quantum yield of **L** are obviously increased. The fluorescence quenching of **L** bound with Hg^{2+} may arise from the heavy-metal effect. In addition, the decreased coplanar effect of Hg_2L_2 will also lead to fluorescence quenching.

dx.doi.org/10.1021/ic200181p |*Inorg. Chem.* 2011, 50, 6543–6551

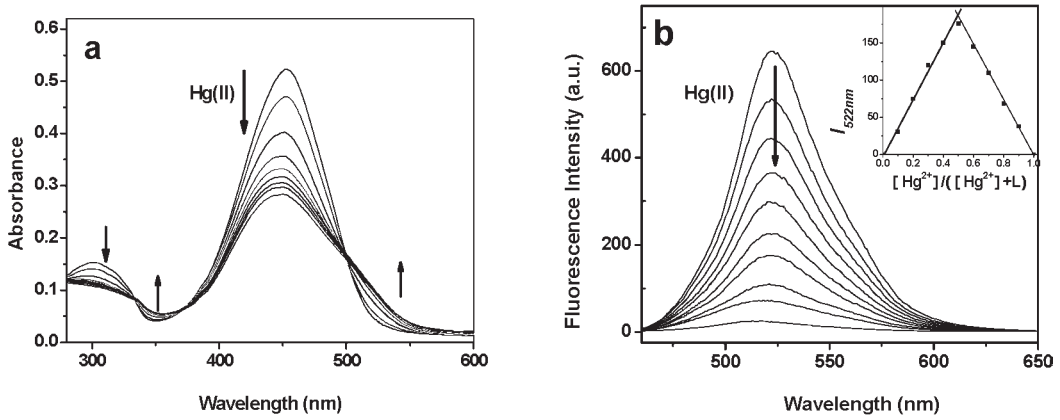

Figure 3. (a) UV−vis absorption titration spectra of **L** (10 μM) in DMSO/H_2O (1:99, v/v) upon the addition of Hg^{2+} (1, 2, 3, 4, 5, 6, 8, 10, 12, 15, and 20 μM, respectively). (b) Fluorescence titration spectra of **L** (10 μM) in DMSO/H_2O (1:99, v/v) upon the addition of Hg^{2+} (0, 1, 2, 3, 4, 5, 6, 7, 8, and 10 μM, respectively). Excitation wavelength: 450 nm. Inset: Job's plot analysis of **L** with Hg^{2+}.

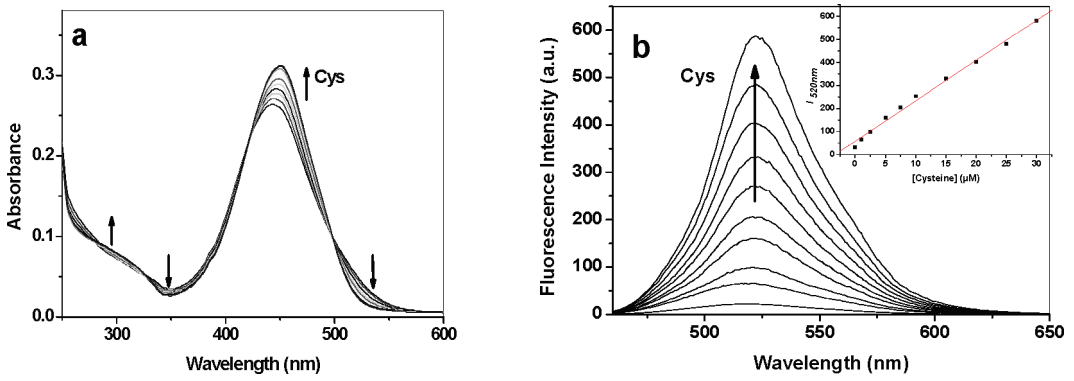

Figure 4. (a) Absorption spectra of $\mathbf{Hg_2L_2}$ (5 μM) in DMSO/H_2O (1:99, v/v) upon the gradual addition of Cys (0, 5, 10, 15, 20, 25, 30, 35, 40, 45, and 50 μM, respectively). (b) Fluorescence spectra of $\mathbf{Hg_2L_2}$ (5 μM) in DMSO/H_2O (1:99, v/v) upon the gradual addition of Cys (0, 1, 2.5, 5, 7.5, 10, 15, 20, 25, and 30 μM, respectively). Excitation wavelength: 450 nm. Inset: Fluorescence intensity of $\mathbf{Hg_2L_2}$ (5 μM) at 520 nm versus the concentration of Cys added.

The addition of mercapto biomolecules such as Cys, Hcy, or GSH to the aqueous solution of $\mathbf{Hg_2L_2}$ resulted in obvious spectral changes. UV−vis absorption and fluorescence spectra of $\mathbf{Hg_2L_2}$ in aqueous solution gradually returned to those characteristic of free **L** when titrated with Cys (Figure 4). An obvious fluorescence increase (about 30-fold) was observed, and the fluorescence quantum yield could be revived to 0.49, indicating that $\mathbf{Hg_2L_2}$ could be applied as a fluorescent *OFF−ON* probe for Cys in aqueous solution. The absorption and fluorescence spectra of $\mathbf{L}/\mathbf{Hg_2L_2}$ clearly illustrate that the addition of Cys results in a complete release of **L** from $\mathbf{Hg_2L_2}$, and the fluorescence is thus recovered, which is also confirmed from the crystal structures.

Interestingly, the alternate addition of a constant amount of Cys and Hg^{2+} to the aqueous solution of $\mathbf{Hg_2L_2}$ gives rise to a switchable change in the fluorescence intensity at 525 nm. Such a reversible interconversion of $\mathbf{Hg_2L_2}/\mathbf{L}$ can be repeated more than 10 times by the modulation of Cys/Hg^{2+} added, indicating that $\mathbf{Hg_2L_2}$ can be developed as a reversible fluorescence *OFF−ON* probe for Cys. Their corresponding fluorescence and visual color changes were also shown in Figure 5. Reversible interconversions between $\mathbf{Hg_2L_2}$ and **L** upon modulation of Cys/Hg^{2+} are illustrated in Figure 6.

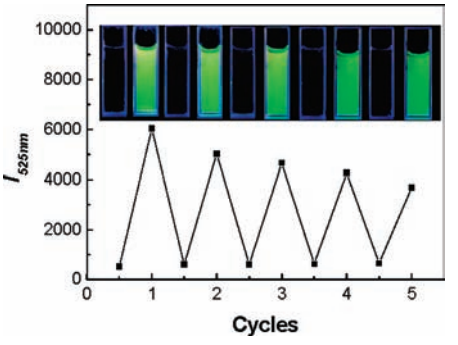

Figure 5. Fluorescent intensity of $\mathbf{Hg_2L_2}$ (5 μM) in DMSO/H_2O (1:99, v/v, 10 mM Tris-HCl, pH = 7.4) upon the alternate addition of Cys/$HgCl_2$ with several concentrations (0:0, 10:0, 10:15, 20:15, 20:30, 40:30, 40:60, 60:60, 60:90, and 100:90 μM, respectively). Excitation at 420 nm. Inset: Their corresponding fluorescence profiles.

^{1}H NMR and ESI-MS Studies. The conversion of $\mathbf{Hg_2L_2}/\mathbf{L}$ was also verified from ^{1}H NMR titration spectra (Figure S1 in the Supporting Information). The proton chemical shifts of the coumarin ring in **L** were distinctly shifted downfield upon the

dx.doi.org/10.1021/ic200181p |*Inorg. Chem.* 2011, 50, 6543–6551

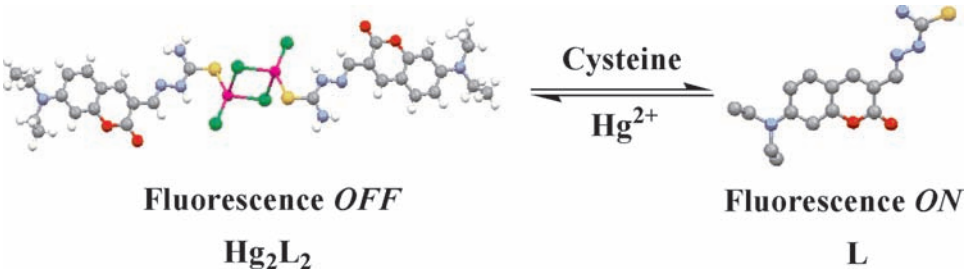

Figure 6. Reversible interconversions between Hg_2L_2 and **L** upon modulation of Cys/Hg^{2+} Color code: pale, H; gray, C; red, O; blue, N; yellow, S; green, Cl; pink, Hg).

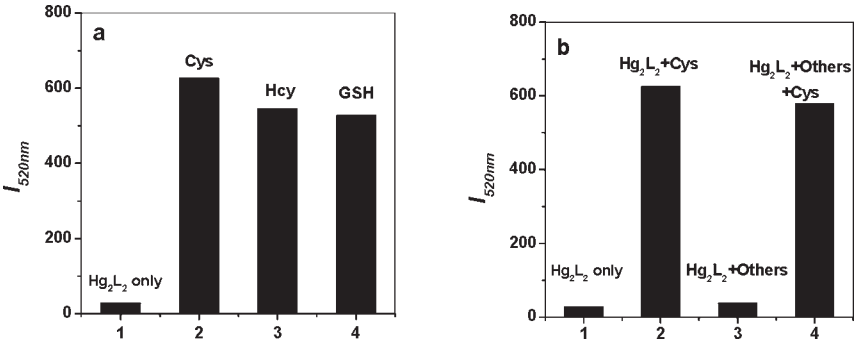

Figure 7. Fluorescent intensity of Hg_2L_2 (5 μM) at 525 nm in DMSO/H_2O (1:99, v/v) (a) with the addition of Cys, Hcy, and GSH (10 μM each) and (b) with the addition of (1) none, (2) 10 μM Cys, (3) other amino acids including glycine, alanine, valine, leucine, isoleucine, methionine, proline, tyrosine, lysine, histidine, serine, and tryptophan (each 10 μM), and (4) 10 μM Cys in the presence of other amino acids.

addition of 2 equiv of $HgCl_2$ and returned to the original values with the subsequent addition of 2.5 equiv of Cys. This reversible interaction was further evidenced by ESI-MS detection of a mixed solution. The peak at m/z 1182.7 corresponding to $[Hg_2L_2 + H]^+$ (calcd m/z 1180.9) was found after 1 equiv of $HgCl_2$ was added to the aqueous solution of **L** (Figure S2 in the Supporting Information), and the peak at m/z 443.0 corresponding to $[2Cys + Hg^{2+}\text{-}H]^+$ (calcd m/z 442.9) was observed upon the addition of 2 equiv of Cys (Figure S3 in the Supporting Information). Thus, ^1H NMR and ESI-MS results firmly support the conclusion that the interconversion of Hg_2L_2/**L** can be modulated by the decomplexation/complexation interaction upon the addition of Cys/Hg^{2+}.

Quantitative Determination of Cys. Both **L** and Hg_2L_2 exhibit excellent water solubility and biocompatibility, as well as good stability under a wide pH span from 6 to 10 covering physiological conditions (Figure S4 in the Supporting Information). These features of **L** and Hg_2L_2 facilitate their practical applications for the determination of Cys. Hg_2L_2 displays a high sensitivity to Cys (the reaction can be completed within several seconds), which can be used to create a calibration curve for a quick quantitative measurement of Cys. Therefore, Cys was added at different concentrations from 0 to 30 μM, and the fluorescence intensity of Hg_2L_2 (5.0 μM) at 525 nm was recorded to generate a calibration curve. A good linearity (R = 0.995) was found between the fluorescence intensity of the solution and the Cys concentration (inset of Figure 4b). This linear fitting analysis reveals that Hg_2L_2 is suitable for determining Cys from 0.5 to 30 μM. When constant amounts of Cys (10 μM) and $HgCl_2$ (10 μM) were alternatively added to an aqueous solution of Hg_2L_2, the fluorescence intensity at 525 nm varied with alternating increases and decreases to over 95%. Such reversible interconversions between

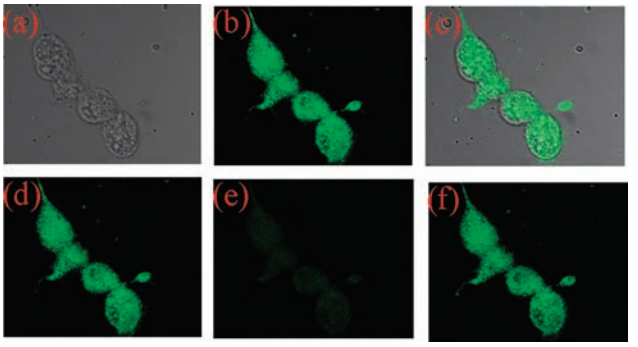

Figure 8. Confocal images of HEK 293 cell lines. Upper panel: (a) Bright-field image; (b) fluorescence imaging after incubation with **L** [10 μM, H_2O/DMF (7:3, v/v), 50 mM Tris-HCl, pH = 7.4] for 15 min; (c) overlay of the bright-field and fluorescent images. Lower panel: Fluorescence imaging of (d) HEK 293 cells after incubation with **L** (10 μM), (e) HEK 293 cells in part d after treatment with $HgCl_2$ (100 μM) for 12 min, and (f) HEK 293 cells in part e after incubation with Cys (200 μM) for 12 min.

Hg_2L_2 and **L** can be repeated in at least five cycles by modulation of the Cys and Hg^{2+} added. Their corresponding fluorescence changes are also given in Figure 5.

High Selectivity to Mercapto Biomolecules. With the exception of Cys, other mercapto biomolecules such as Hcy and GSH also induced similar variations in the absorption and fluorescence spectra of Hg_2L_2. Among these, Cys led to the largest fluorescence increase, whereas Hcy and GSH gave relatively smaller increases in fluorescence (Figure 7a). For practical applications, an important consideration is its selective detection in the presence of other amino acids without thiol groups, such as glycine, alanine, valine,

leucine, isoleucine, methionine, proline, tyrosine, lysine, histidine, serine, and tryptophan. As shown in Figure 7b, the addition of other competitive amino acids to the solution of $\mathbf{Hg_2L_2}$ did not result in any notable fluorescent increases. However, when Cys was added to the aqueous solution of $\mathbf{Hg_2L_2}$ containing other competitive amino acids, an obvious increase in fluorescence was observed. This result indicates that $\mathbf{Hg_2L_2}$ can detect Cys with a high selectivity over other coexisting amino acids.

Cell Culture. The foreign uptake of mercapto biomolecules in HEK293 cells (human embryotic kidney cell, without thiols) and intracellular mercapto biomolecules in SYS5 cells (human neuroblastoma SH cell) was examined using confocal fluorescence imaging. As shown in Figure 8, HEK293 cell lines after incubation with **L** (10 μM) for 15 min were conveniently imaged using a confocal fluorescence microscope. The matched fluorescence and bright-field images elicited the intracellular uptake of **L** by HEK293 cells (Figure 8a−c). The HEK 293 cells incubated with **L** (10 μM; Figure 8d) were treated with $HgCl_2$ (100 μM) for 12 min. Their fluorescence images became dim (Figure 8e), implying that the intracellular uptake of Hg^{2+} ions complexed with **L** yielded nonfluorescent $\mathbf{Hg_2L_2}$. Upon further incubation of these cells with foreign uptake of Cys (200 μM) for 12 min, green fluorescence imaging was recovered (Figure 8f). The recurrent imaging indicated that the uptake of Cys resulted in the decomplexation of intracellular $\mathbf{Hg_2L_2}$ to fluorescent **L**. Through reversible fluorescence imaging, intracellular interconversion of $\mathbf{Hg_2L_2}$/**L** was explicitly illustrated. Therefore, the *ON*−*OFF*−*ON* fluorescence imaging of **L** was accomplished in HEK293 cell lines by the intracellular complexation/decomplexation interaction modulated by Hg^{2+}/Cys.

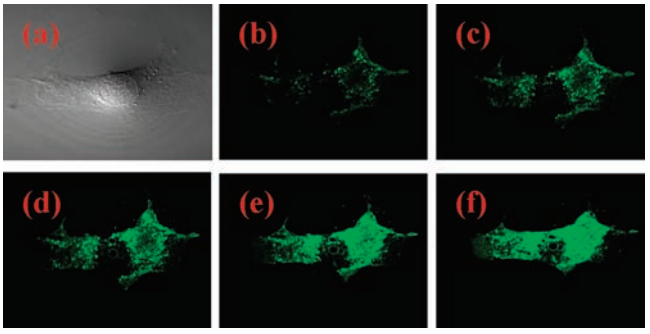

Figure 9. Confocal images of SYS5 cell lines. Bright-field image (a) and fluorescence images after incubation with $\mathbf{Hg_2L_2}$ [10 μM, H_2O/DMF (7:3, v/v), 50 mM Tris-HCl, pH = 7.4] for 1 min (b), 3 min (c), 6 min (d), 9 min (e), and 15 min (f).

Intracellular thiol-enriched cells such as SYS5 also induced nonfluorescent $\mathbf{Hg_2L_2}$ to give distinct fluorescence imaging like Cys did (Figure 9). After SYS5 cell lines were incubated with $\mathbf{Hg_2L_2}$ (10 μM) for 1 min, referring to its bright-field image (Figure 9a), only a weak fluorescence emission was imaged in certain loci of the cell (Figure 9b). After 6 min, the intensity of imaged fluorescence emission increased and the area expanded (Figure 9d). After 15 min, the bright emission from the whole cell was imaged (Figure 9f). Likewise, the initially weak fluorescence emission originated from the decomplexation of $\mathbf{Hg_2L_2}$ in the thiol-enriched portion of the SYS5 cells. As the incubation time increased, the concentration of intracellular **L** increased and subsequently the concentrated **L** diffused to the whole cell, analogous to the uptake of free **L** in HEK293 cells. These results indicate that intracellular fluorescent recurrence could also be accomplished by thiol-enriched cells instead of foreign Cys, which provides the possibility of exploring the self-detoxification process of Hg^{2+} ions in living cells.

On the basis of the result of confocal fluorescence imaging above, a pair of sensors, **L**/$\mathbf{Hg_2L_2}$, was further used to illustrate the intracellular self-detoxification process by the toxic uptake of Hg^{2+} ions (Figure 10). The SYS5 cell lines incubated with $\mathbf{Hg_2L_2}$ (10 μM) for 10 min were treated with $HgCl_2$ (10 μM; entry 1).

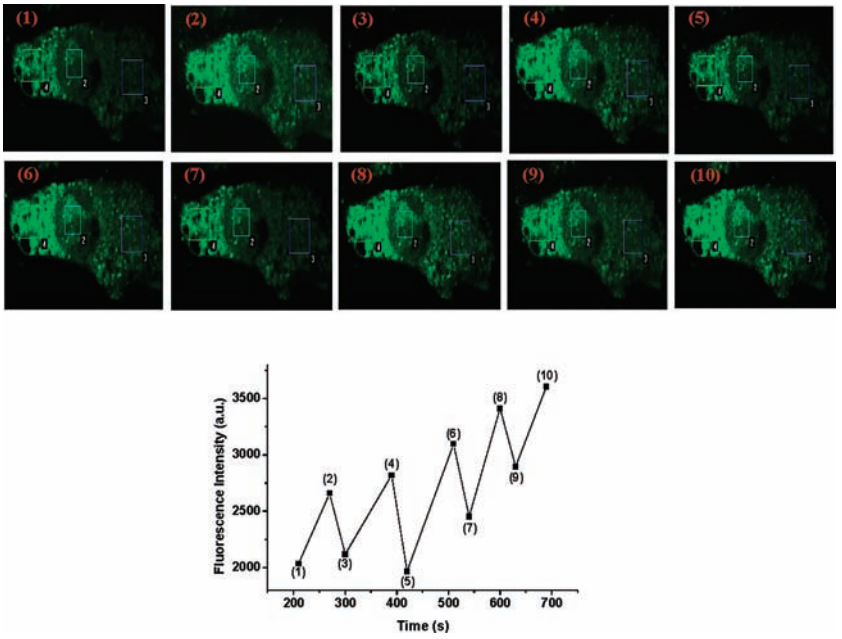

Figure 10. Confocal fluorescence imaging in the SYS5 cell lines incubated with $\mathbf{Hg_2L_2}$ [10 μM, H_2O/DMF (7/3, v/v), 50 mM Tris-HCl, pH = 7.4] upon the multistep addition of $HgCl_2$ (10 μM each) with regular time intervals (entries 1−10). Upper: In situ determination of their fluorescence imaging (fluorescence changes of region 4 were recorded for comparison). Lower: Their corresponding changes in the fluorescence intensity with time.

dx.doi.org/10.1021/ic200181p |*Inorg. Chem.* 2011, 50, 6543–6551

With increasing incubation time, the intracellular fluorescence intensity was enhanced because the strongly fluorescent **L** (released from $\mathbf{Hg_2L_2}$) diffused to the whole cell (entry 2). With continued treatment of the SYS5 cell lines above with $HgCl_2$ (10 μM), their fluorescence images became dim quickly (entry 3). Surprisingly, after about 2 min, the intracellular fluorescence was revived to its original intensity again (entry 4). We repeated such experiments to find that the intracellular fluorescent decreases (entries 1, 3, 5, 7, and 9) and increases (entries 2, 4, 6, 8, and 10) could be recurrent at least 10 times. For illustration of an alternate fluorescence variation, the in situ determination of their corresponding fluorescence in vivo in the SYS5 cell lines was also shown in Figure 10. Obviously, the reversible intracellular fluorescence revival upon the multistep addition of $HgCl_2$ was relevant to the increase of the intracellular active mercapto biomolecules. As we know from cell biology, upon intracellular uptake of some toxic species such as Hg^{2+} ions, the cells will start the transduction and expression of antigene, and those detox species are biosynthesized and secreted into the cells. SYS5, as a kind of intracellular thiol-enriched cells, can always secrete mercapto biomolecules for Hg^{2+} complexation when the toxic Hg^{2+} ions are added repeatedly. These mercapto biomolecules can form a stable complex with Hg^{2+} ions and excrete out of the cells via metabolism to complete a self-detoxification process. Therefore, $\mathbf{L}/\mathbf{Hg_2L_2}$ can be applied to track the intracellular self-detoxification process, which will give a simple and convenient method to study the cell toxicity. This also provides a new way of communicating with living systems and adjusting and controlling the chemical species inside cells that are critical for intracellular engineering, manipulation, and the probe.[19]

4. CONCLUSIONS

In summary, a coumarin-derived imine (**L**) was synthesized and its complex, $\mathbf{Hg_2L_2}$, was developed as a reversible fluorescent probe for selective sensing of mercapto biomolecules such as Cys, Hcy, and GSH. $\mathbf{Hg_2L_2}$ exhibited a series of advantages as fluorescent probes including highly sensitive detection, fluorescence *OFF*−*ON*, reversible interconversion, good water solubility, high quantum yield of **L** (0.50), longer emission wavelength (525 nm), and a wide pH span (6−10). The interconversion of $\mathbf{Hg_2L_2}$ and **L** in aqueous solution via the decomplexation/complexation was definitely verified from crystal structures and ESI-MS, NMR, UV−vis, and fluorescence spectra. Confocal fluorescence imaging in the SYS5 cells reveals that $\mathbf{L}/\mathbf{Hg_2L_2}$ can be applied to monitor the intracellular self-detoxification process to avoid toxic intracellular uptake. This will provide a new strategy for the design of reversible fluorescent probes to study the self-detoxification mechanism of heavy metals in living cells.

■ ASSOCIATED CONTENT

Supporting Information. X-ray crystallographic data of ligand **L** and complex $\mathbf{Hg_2L_2}$ in CIF format, additional spectra, NMR copies, and visual fluorescence imaging. This material is available free of charge via the Internet at http://pubs.acs.org.

■ AUTHOR INFORMATION

Corresponding Author
*E-mail: wangpf@mail.ipc.ac.cn.

■ ACKNOWLEDGMENT

This work was supported by the National Natural Science Foundation of China (Grants 20953002, 20903110, and 60978034), the Research Grants Council of the Hong Kong SAR (Project CityU 123607), and the National Basic Research Program of China (Grant 2007CB936001).

■ REFERENCES

(1) Shahrokhian, S. *Anal. Chem.* **2001**, *73*, 5972–5978.

(2) (a) Seshadri, S.; Beiser, A.; Selhub, J.; Jacques, P. F.; Rosenberg, I. H.; D'Agostino, R. B.; Wilson, P. W.; Wolf., P. A. *N. Engl. J. Med.* **2002**, *346*, 476–483. (b) Ueland, P. M.; Vollset, S. E. *Clin. Chem.* **2004**, *50*, 1293–1295.

(3) (a) Hassan, S. S. M.; Rechnitz, G. A. *Anal. Chem.* **1982**, *54*, 1972–1976. (b) Hwang, C.; Sinskey, A. J.; Lodish, H. F. *Science* **1992**, *257*, 1496–1502. (c) Hong, R.; Han, G.; Fernandez, J. M.; Kim, B.-J.; Forbes, N. S.; Rotello, V. M. *J. Am. Chem. Soc.* **2006**, *128*, 1078–1079.

(4) Guan, X.; Hoffman, B.; Dwivedi, C.; Matthees, D. P. *J. Pharm. Biomed. Anal.* **2003**, *31*, 251–261.

(5) Capitan, P.; Malmezat, T.; Breuille, D.; Obled, C. *J. Chromatogr., B: Biomed. Sci. Appl.* **1999**, *732*, 127–135.

(6) Qian, X.-X.; Nagashima, K.; Hobo, T.; Guo, Y.-Y.; Yamaguchi, C. *J. Chromatogr., A* **1990**, *515*, 257–264.

(7) (a) Melnyk, S.; Pogribna, M.; Pogribny, I.; Hine, R. J.; James, S. J. *J. Nutr. Biochem.* **1999**, *10*, 490–497. (b) Hiraku, Y.; Murata, M.; Kawanishi, S. *Biochim. Biophys. Acta* **2002**, *1570*, 47–52.

(8) (a) Wang, W.; Rusin, O.; Xu, X.; Kim, K. K.; Escobedo, J. O.; Fakayode, S. O.; Fletcher, K. A.; Lowry, M.; Schowalter, C. M.; Lawrence, C. M.; Fronczek, F. R.; Warner, I. M.; Strongin, R. M. *J. Am. Chem. Soc.* **2005**, *127*, 15949–15958. (b) Li, H.; Fan, J.; Wang, J.; Tian, M.; Du, J.; Sun, S.; Sun, P.; Peng, X. *Chem. Commun.* **2009**, 5904–5906. (c) Maeda, H.; Matsuno, H.; Ushida, M.; Katayama, K.; Saeki, K.; Itoh, N. *Angew. Chem., Int. Ed.* **2005**, *44*, 2922–2925. (d) Kim, T.-K.; Lee, D.-N.; Kim, H.-J. *Tetrahedron Lett.* **2008**, *49*, 4879–4881. (e) Lin, W. Y.; Long, L. L.; Yuan, L.; Cao, Z. M.; Chen, B. B.; Tan, W. *Org. Lett.* **2008**, *10*, 5577–5580. (f) Lee, K. S.; Kim, T. K.; Lee, J. H.; Kim, H. J.; Hong, J. I. *Chem. Commun.* **2008**, 6173–6175. (g) Zhang, X. J.; Ren, X. S.; Xu, Q. H.; Loh, K. P.; Chen, Z. K. *Org. Lett.* **2009**, *11*, 1257–1260. (h) Wang, W.; Escobedo, J. O.; Lawrence, C. M.; Strongin, R. M. *J. Am. Chem. Soc.* **2004**, *126*, 3400–3401. (i) Chen, X.; Zhou, Y.; Peng, X.; Yoon, J. *Chem. Soc. Rev.* **2010**, *39*, 2120–2135. (j) Chen, X.; Ko, S.-K.; Kim, M. J.; Shin, I.; Yoon, J. *Chem. Commun.* **2010**, *46*, 2751–2753.

(9) (a) Berezin, M. Y.; Achilefu, S. *Chem. Rev.* **2010**, *110* 2641–2684. (b) Lee, J. H.; Lim, C. S.; Tian, Y. S.; Han, J. H.; Cho, B. R. *J. Am. Chem. Soc.* **2010**, *132*, 1216–1217. (c) Bouffard, J.; Kim, Y.; Swager, T. M.; Weissleder, R.; Hilderbrand, S. A. *Org. Lett.* **2008**, *10*, 37–40. (d) Tang, B.; Xing, Y.; Li, P.; Zhang, N.; Yu, F.; Yang, G. *J. Am. Chem. Soc.* **2007**, *129*, 11666–11667. (e) Zhang, M.; Yu, M.; Li, F.; Zhu, M.; Li, M.; Gao, Y.; Li, L.; Liu, Z.; Zhang, J.; Zhang, D.; Yi, T.; Huang, C. *J. Am. Chem. Soc.* **2007**, *129*, 10322–10323.

(10) (a) Zheng, H.; Qian, Z.-H.; Xu, L.; Yuan, F.-F.; Lan, L.-D.; Xu, J.-G. *Org. Lett.* **2006**, *8*, 859–861. (b) Wu, J.-S.; Hwang, I.-C.; Kim, K. S.; Kim, J. S. *Org. Lett.* **2007**, *9*, 907–910. (c) Xiang, Y.; Tong, A.; Jin, P.; Ju, Y. *Org. Lett.* **2006**, *8*, 2863–2866. (d) Yang, Y.-K.; Yook, K.-J; Tae, J. *J. Am. Chem. Soc.* **2005**, *127*, 16760–16761. (e) Xiang, Y.; Tong, A. *Org. Lett.* **2006**, *8*, 1549–1552. (f) Kwon, J. Y.; Jang, Y. J.; Lee, Y. J.; Kim, K. M.; Seo, M. S.; Nam, W.; Yoon, J. *J. Am. Chem. Soc.* **2005**, *127*, 10107–10111. (g) Dujols, V.; Ford, F.; Czarnik, A. W. *J. Am. Chem. Soc.* **1997**, *119*, 7386–7387. (h) Kim, H. N.; Lee, M. H.; Kim, H. J.; Kim, J. S.; Yoon, J. *Chem. Soc. Rev.* **2008**, *37*, 1465–1472. (i) Chen, X.; Nam, S.-W.; Jou, M. J.; Kim, Y.; Kim, S.-J.; Park, S.; Yoon, J. *Org. Lett.* **2008**, *10*, 5235–5238.

(11) (a) Wallace, K. J.; Fagbemi, R. I.; Folmer-Andersen, F. J.; Morey, J.; Lyntha, V. M.; Anslyn, E. V. *Chem. Commun.* **2006**, 3886–3888.

(b) Dahiya, P.; Kumbhakar, M.; Maity, D. K.; Mukherjee, T.; Mittal, J. P.; Tripathi, A. B. R.; Chattopadhyay, N.; Pal, H. *Photochem. Photobiol. Sci.* **2005**, *4*, 100–105. (c) Murata, C.; Masuda, T.; Kamochi, Y.; Todoroki, K.; Yoshida, H.; Nohta, H.; Yamaguchi, M.; Takadate, A. *Chem. Pharm. Bull.* **2005**, *53*, 750–758. (d) Kim, H. M.; Yang, P. R.; Seo, M. S.; Yi, J.-S.; Hong, J. H.; Jeon, S.-J.; Ko, Y.-G.; Lee, K. J.; Cho, B. R. *J. Org. Chem.* **2007**, *72*, 2088–2096.

(12) (a) Hagen, V.; Dekowski, B.; Nache, V.; Schmidt, R.; Geibler, B.; Lorenz, D.; Eichhorst, J.; Keller, S.; Kaneko, H.; Benndorf, K.; Wiesner, B. *Angew. Chem., Int. Ed.* **2005**, *44*, 7887–7891. (b) Secor, K. E.; Glass, T. E. *Org. Lett.* **2004**, *6*, 3727–3730. (c) Akita, S.; Umezawa, N.; Higuchi, T. *Org. Lett.* **2005**, *7*, 5565–5568. (d) Hirano, T.; Hiromoto, K.; Kagechika, H. *Org. Lett.* **2007**, *9*, 1315–1318. (e) Wang, J.; Xie, J.; Schultz, P. G. *J. Am. Chem. Soc.* **2006**, *128*, 8738–8739. (f) Chattopadhyay, N.; Mallick, A.; Sengupta, S. *J. Photochem. Photobiol. A* **2006**, *177*, 55–60. (g) Gawley, R. E.; Shanmugasundarama, M.; Thorne, J. B.; Tarkk, R. M. *Toxicon* **2005**, *45*, 783–787.

(13) Wu, J.; Liu, W.; Zhuang, X.; Wang, F.; Wang, P.; Tao, S.; Zhang, X. H.; Wu, S.; Lee, S. *Org. Lett.* **2007**, *9*, 33–36.

(14) Sheldrick, G. M. *Acta Crystallogr., Sect. A* **2008**, *64*, 112–122.

(15) (a) Paeker, C. A.; Rees, W. T. *Analyst* **1960**, *85*, 587–600. (b) Gabe, T.; Urano, Y.; Kikuchi, K.; Kojima, H.; Nagano, T. *J. Am. Chem. Soc.* **2004**, *126*, 3357–3367.

(16) (a) Schwarzenbach, G. In *Soft and Hard Acids and Bases*; Pearson., R. G., Ed.; John Wiley: New York, 1973; p 20. (b) Kolthoff, I. M. *Treatise Anal. Chem.* **1979**, 129.

(17) (a) Nolan, E. M.; Burdette, S. C.; Harvey, J. H.; Hilderbrand, S. A.; Lippard, S. J. *Inorg. Chem.* **2004**, *43*, 2624–2635. (b) Nolan, E. M.; Lippard, S. J. *Inorg. Chem.* **2004**, *43*, 8310–8317. (c) Nolan, E. M.; Lippard, S. J. *J. Am. Chem. Soc.* **2003**, *125*, 14270–14271.

(18) (a) Coskun, A.; Deniz, E.; Akkaya, E. U. *Org. Lett.* **2005**, *7*, 5187–5189. (b) Coskun, A.; Akkaya, E. U. *J. Am. Chem. Soc.* **2006**, *128*, 14474–14475.

(19) Win, M. N.; Smolke, C. D. *Science* **2008**, *322*, 456–460.